Birefringence in Crystalline Mirror Coatings v.8

M. M. Fejer
November 25, 2020

1. Introduction

While the dielectric tensor is isotropic in cubic materials like AlGaAs, the fourth-rank photoelastic tensor is not, which influences the form that the birefringence induced by thermal stresses will take. It is the purpose of this note to illustrate some aspects of thermoelastic birefringence in AlGaAs coatings.

1.1. Summary of the results

For a total absorbed power P_{abs} distributed as a Gaussian of $1/e^2$ radius w in a thin multilayer mirror of cubic symmetry on a thick substrate, simplified for the case where the square of the photoelastic asymmetry parameter $A \equiv 2p_{44}/(p_{11}-p_{12})$ is large ($A^2 = 33$ in GaAs), the difference between the reflection phase for light polarized along the two principal birefringent axes is given by [Eq. (6.12)]

$$B_m(R \equiv r/w) = B_{0m}\left[\frac{\alpha_s}{\alpha}(1+\nu_s)f_s(R) + f_m(R)\right]\sin 2\theta \tag{1.1}$$

where

$$B_{0m} \equiv -\sqrt{\frac{\pi}{2}}\frac{p_{44}\alpha}{k_s}\frac{P_{abs}}{w}\left(\frac{n_L/n_H}{1-(n_L/n_H)^2}\right)\left[n_H^2 n_L + n_L^2 n_H\right] \tag{1.2}$$

and the p_{IJ} are photoelastic tensor components, n_H and n_L are the refractive index of the high and low index layers, respectively, α and α_s are the thermal expansion coefficients of the mirror (assumed the same in the high and low index layers) and the substrate, respectively, k_s is the thermal conductivity of the substrate, ν_s is the substrate Poisson ratio, and θ is the angle with respect to the crystalline **x** axis of the coating, assumed to be oriented with the **z** axis normal to the mirror surface. The functions $f_m(R)$ and $f_s(R)$ defined in Eqs. (5.13), are plotted below

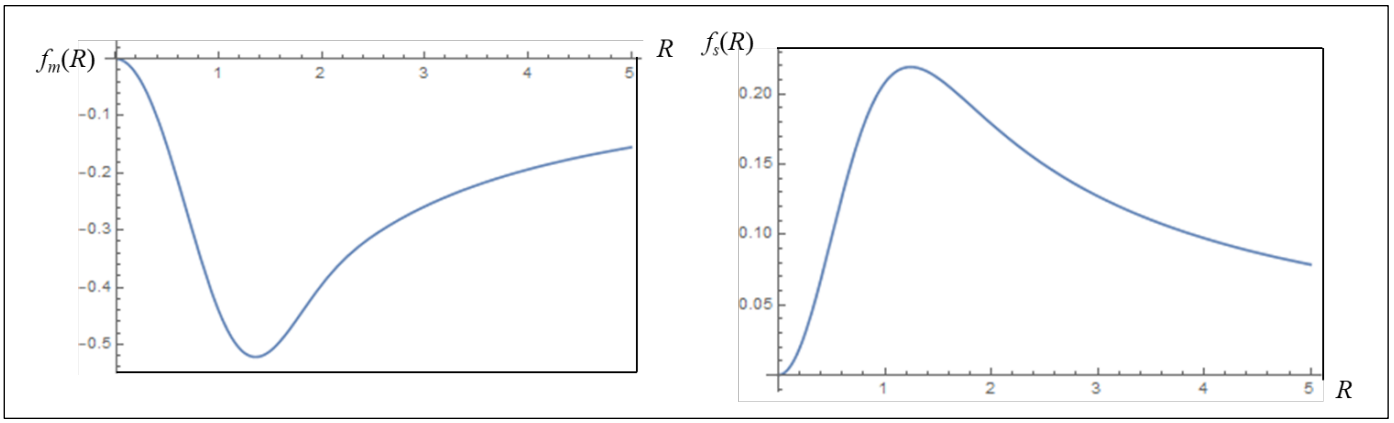

For an AlGaAs mirror (x = 0.9 and x = 0.1 assumed) on a silica substrate, the prefactor B_{0m} is given by Eq. (6.14)

$$B_{0m} = 8.9\times10^{-3}\,\frac{P_{abs}[\mathrm{W}]}{w[\mathrm{cm}]} \tag{1.3}$$

We see that for 5 W absorbed from a 5 cm radius beam, the maximum birefringent phase will be 4.5 mrad. Using the same scaling, if there were an absorber of 0.5 mm in size, it would create a birefringence of ~450 mrad per watt of absorbed power. Because of the weak (only $1/r$) rolloff of the birefringence away from the absorber, a larger area than that of the absorber itself would be affected.

If irregularly distributed birefringence is introduced into the mirror during growth or bonding, there is no *a priori* way to predict the expected birefringent phase on reflection unless the irregular strains are known. Conversely, if measurements of the local birefringent phase and principal axes are available, the principal components and axes of the strain can be computed with the results of section 6.5.2, which may be of use in diagnosing the origin of the strains. The connection of the strain to birefringence in reflection for a general orientation of the principal birefringent axes is given in Eq. (6.16). For principal birefringence axes along the [011] direction for the same AlGaAs mirror considered in Eq. (1.3) the principal strain axes are in that same direction, and the result for their magnitude reduces to

$$\left|\tilde{S}_1 - \tilde{S}_2\right|_p = 9.3\times10^{-6}\,B_m[\mathrm{mrad}] \tag{1.4}$$

The corresponding difference in principal stresses is [Eq. (6.17)]

$$\left|\tilde{T}_1 - \tilde{T}_2\right|_p = 1.1\,\mathrm{MPa}\,B_m[\mathrm{mrad}] \tag{1.5}$$

1.2. Outline of the calculation

Section 2 outlines the formal description of photoelasticity, and computes the refractive index change and the birefringence induced in a thin layer, given specified elastic strains in that layer. Section 3 outlines the changes necessary to include thermoelasticity in the calculation, and relates the strains in an object of cylindrical symmetry to the Cartesian tensor components required for photoelastic computations. Section 4 considers the case of a thin layer of cubic symmetry on thick substrate. Section 5 applies the method to two cases, in 5.1 a layer on a substrate with uniform temperature change, and in 5.2 a Gaussian radial distribution of heat deposited on its surface, and shows some simplifications in highly photoelastically anisotropic materials like GaAs. The evaluation of built-in strains from measurements of the static birefringence are also given in Section 5.3. Section 6 relates the birefringence of the reflection phase of a mirror to the birefringence changes in each layer of the mirror, and computes the results for an AlGaAs mirror. Section 7 addresses possible extensions of the present calculation and related future work. Section 8 is an Appendix listing pertinent material properties.

2. Photoelasticity in cubic materials

2.1. Photoelastic tensor

Photoelasticity is generally formulated in terms of the impermeability tensor $\mathbf{b} \equiv \boldsymbol{\varepsilon}^{-1}$. For a strain field $\mathbf{S}_J$ in Voight notation, the perturbation to the impermeabiltiy tensor is given by the photoelastic tensor $\mathbf{p}$

$$\Delta \mathbf{b}_I = \mathbf{p}_{IJ} \mathbf{S}_J \tag{2.1}$$

Since $\mathbf{p}$ relates two second rank tensors, it is a fourth rank tensor, and has the same symmetry as the stiffness tensor $\mathbf{c}$. For a cubic material, we have

$$\mathbf{p} = \begin{bmatrix} p_{11} & p_{12} & p_{12} & 0 & 0 & 0 \\ p_{12} & p_{11} & p_{12} & 0 & 0 & 0 \\ p_{12} & p_{12} & p_{11} & 0 & 0 & 0 \\ 0 & 0 & 0 & p_{44} & 0 & 0 \\ 0 & 0 & 0 & 0 & p_{44} & 0 \\ 0 & 0 & 0 & 0 & 0 & p_{44} \end{bmatrix} \tag{2.2}$$

In an isotropic material there is the additional constraint that $p_{44} = (p_{11} - p_{12})/2$. The anisotropy of the photoelastic response is often characterized by the anisotropy factor

$$A \equiv \frac{2p_{44}}{p_{11} - p_{12}} \tag{2.3}$$

which equals unity in isotropic materials, and with the data in Appendix 1 takes the value 5.76 in GaAs.

2.2. Refractive index perturbation

2.2.1. Perturbed impermeability tensor

For propagation along the $\mathbf{z}$ axis, the $\mathbf{x}$ and $\mathbf{y}$ components of the dielectric (and hence impermeability) tensor are pertinent. In the principal axis frame of this subtensor $\mathbf{b}_\perp$, the refractive index for light polarized along a principal axis direction is the square root of the reciprocal of the corresponding diagonal tensor component.

From Eqs. (2.1) and (2.2) we have for $\mathbf{b}_\perp$, now in conventional tensor form

$$\mathbf{b}_\perp = \begin{bmatrix} b_1 & b_6 \\ b_6 & b_2 \end{bmatrix} \tag{2.4}$$

where

$$\begin{aligned} b_1 &= n^{-2} + p_{11}S_1 + p_{12}(S_2 + S_3) \\ b_2 &= n^{-2} + p_{11}S_2 + p_{12}(S_1 + S_3) \\ b_6 &= n^{-2} + p_{44}S_6 \end{aligned} \tag{2.5}$$

2.2.2. Diagonalization, birefringence, principal axes

Call the two principal components of the symmetric two by two matrix in Eq. (2.5) b_+, b_-. Diagonalizing Eq. (2.4) we have

$$b_\pm = \left[b_1 + b_2 \pm \sqrt{(b_1 - b_2)^2 + 4b_6^2} \right] / 2 \tag{2.6}$$

With Eqs. (2.5) and (2.6), we have

$$\begin{aligned} &\varepsilon_\pm = b_\pm^{-1} \\ &\Rightarrow n_\pm = \sqrt{\varepsilon_\pm} \approx n - \frac{n^3}{2}\left\{ \left[(p_{11} + p_{12})(S_1 + S_2) + 2p_{12}S_3 \right] \pm \sqrt{(p_{11} - p_{12})^2 (S_1 - S_2)^2 + 4p_{44}^2 S_6^2} \right\} \end{aligned} \tag{2.7}$$

and the angle θ_0 between an eigenvector (and thus a principal birefringent axis) and the **x** axis obeys

$$\begin{aligned} \tan 2\theta_0 &= \frac{2b_6}{b_1 - b_2} = \frac{2p_{44}S_6}{(p_{11} - p_{12})(S_1 - S_2)} = A\frac{S_6}{S_1 - S_2} \\ &\xrightarrow[isotropic]{} \frac{S_6}{S_1 - S_2} \end{aligned} \tag{2.8}$$

where the isotropic limits take advantage of the isotropy condition $p_{44} = (p_{11} - p_{12})/2$.

The birefringence is then

$$\begin{aligned} B = n_+ - n_- &= -n^3 \sqrt{(p_{11} - p_{12})^2 (S_1 - S_2)^2 + 4p_{44}^2 S_6^2} \\ &= -n^3 (p_{11} - p_{12}) \sqrt{(S_1 - S_2)^2 + A^2 S_6^2} \\ &\xrightarrow[isotropic]{} -n^3 (p_{11} - p_{12}) \sqrt{(S_1 - S_2)^2 + S_6^2} \end{aligned} \tag{2.9}$$

2.2.3. Comparison of cubic vs isotropic media

It is useful to compare the photoelastic behavior of cubic vs isotropic media. Consider a purely compressional strain along different directions in the medium. Take the displacement to be

$$u_x = S_0 s \cos\theta, u_y = S_0 s \sin\theta \tag{2.10}$$

where $s \equiv \sqrt{x^2 + y^2}$, which could be considered a compression along a direction θ to the **x** axis. The corresponding strains are then

(2.11)

$$
\begin{aligned}
S_1 &= \frac{\partial u_x}{\partial x} = \frac{\partial u_x}{\partial s}\frac{\partial s}{\partial x} = S_0 \cos\theta \frac{x}{s} = S_0 \cos^2\theta \\
S_2 &= S_0 \sin^2\theta \\
S_6 &= \frac{\partial u_x}{\partial y} + \frac{\partial u_y}{\partial x} = 2S_0 \cos\theta \sin\theta
\end{aligned}
\tag{2.12}
$$

Noting that with Eqs. (2.12) $S_1 - S_2 = S_0 \cos 2\theta$ and $S_6 = S_0 \sin 2\theta$, we have for the birefringence from Eq. (2.9)

$$
\begin{aligned}
B &= -S_0 n^3 \sqrt{(p_{11}-p_{12})^2 \cos^2 2\theta + 4p_{44}^2 \sin^2 2\theta} \\
&= -S_0 n^3 (p_{11}-p_{12}) \sqrt{\cos^2 2\theta + A^2 \sin^2 2\theta} \\
&\xrightarrow[isotropic]{} -S_0 n^3 (p_{11}-p_{12})
\end{aligned}
\tag{2.13}
$$

and with Eq. (2.8)the angle of a principal axis is

$$
\begin{aligned}
\tan 2\theta_0 &= \frac{2p_{44}\sin 2\theta}{(p_{11}-p_{12})\cos 2\theta} \equiv A \tan 2\theta \\
&\xrightarrow[isotropic]{} \tan 2\theta \quad \Rightarrow \theta_0 = \theta
\end{aligned}
\tag{2.14}
$$

We see that for an isotropic medium, the magnitude of the birefringence is independent of the in-plane direction of the compression and has a principal axis aligned with the direction of the compression, while these conditions will not hold in general for a cubic medium.

2.2.4.Effect of a free surface

For a thin layer with a stress free surface, we can eliminate S_3, in terms of S_1 and S_2. Recall that

$$
\begin{aligned}
T_3 &= c_{12}(S_1 + S_2) + c_{11} S_3 = 0 \\
&\Rightarrow \; S_3 = -\frac{c_{12}}{c_{11}}(S_1 + S_2)
\end{aligned}
\tag{2.15}
$$

With Eq. (2.15) in Eq. (2.7) for the principal refractive indexes, we find

$$
n_{\pm} = n - \frac{n^3}{2}\left\{\left[p_{11} + p_{12}\left(1 - \frac{2c_{12}}{c_{11}}\right)\right](S_1 + S_2) \pm \sqrt{(p_{11}-p_{12})^2 (S_1 - S_2)^2 + 4p_{44}^2 S_6^2}\right\} \tag{2.16}
$$

We see that the free surface alters the average refractive index change for a specified in-plane dilation $S_1 + S_2$, but does not alter the birefringence from the form given in Eq. (2.9). Noting that $S_{rr} + S_{\theta\theta} = S_1 + S_2$, Eq. (2.16) can be used equally well to include a free surface for cases where cylindrical coordinates are used.

2.3. Axisymmetric strain

For cylindrical objects, the natural coordinate system is generally also cylindrical. For an axisymmetric displacement field

$$\mathbf{u} = u_r \hat{\mathbf{r}} \tag{2.17}$$

the strain fields in the plane normal to *z* are

$$S_{rr} = \frac{du_r}{dr},\ S_{\theta\theta} = \frac{u_r}{r} \tag{2.18}$$

It is more convenient to use rectangular coordinates for the photoelastic calculations. The coordinate transformation yields

$$\begin{aligned}\begin{bmatrix} S_{xx} & S_{xy} \\ S_{xy} & S_{yy} \end{bmatrix} &= \begin{bmatrix} S_{rr}\cos^2\theta + S_{\theta\theta}\sin^2\theta & (S_{rr} - S_{\theta\theta})\cos\theta\sin\theta \\ (S_{rr} - S_{\theta\theta})\cos\theta\sin\theta & S_{rr}\sin^2\theta + S_{\theta\theta}\cos^2\theta \end{bmatrix} \\ &= \begin{bmatrix} (du_r/dr)\cos^2\theta + (u_r/r)\sin^2\theta & (du_r/dr - u_r/r)\cos\theta\sin\theta \\ (du_r/dr - u_r/r)\cos\theta\sin\theta & (du_r/dr)\sin^2\theta + (u_r/r)\cos^2\theta \end{bmatrix}\end{aligned} \tag{2.19}$$

For using these results in photoelastic calculations recall that $S_6 = 2S_{xy}$

2.3.1. Uniform strain

Note that for a uniform radial expansion

$$u_r(r) = S_0 r \hat{\mathbf{r}} \tag{2.20}$$

we find $du_r / dr = u_r / r = S_0$, so that with Eq. (2.19) we find $S_{xx} = S_{yy} = S_0$, $S_{xy} = 0$, independent of θ. With these strains in Eq. (2.9), and recalling that $S_6 = 2S_{xy}$ we see that the birefringence vanishes for a uniform in-in-plane dilation.

3. Thermoelasticity

In a cubic medium including thermal expansion effects requires modifying the constitutive relations for Hook's Law and for the thermo-optic effect to read as

$$\begin{bmatrix} T_1 \\ T_2 \\ T_3 \\ T_4 \\ T_5 \\ T_6 \end{bmatrix} = \begin{bmatrix} c_{11} & c_{12} & c_{12} & & & \\ c_{12} & c_{11} & c_{12} & & & \\ c_{12} & c_{12} & c_{11} & & & \\ & & & c_{44} & & \\ & & & & c_{44} & \\ & & & & & c_{44} \end{bmatrix} \begin{bmatrix} S_1 - \alpha\tau \\ S_2 - \alpha\tau \\ S_3 - \alpha\tau \\ S_4 \\ S_5 \\ S_6 \end{bmatrix}$$

$$\Delta \mathbf{b}_{\mathrm{I}} = \mathbf{p}_{\mathrm{IJ}} \begin{bmatrix} S_1 - \alpha\tau \\ S_2 - \alpha\tau \\ S_3 - \alpha\tau \\ S_4 \\ S_5 \\ S_6 \end{bmatrix} - 2n^{-3} \begin{bmatrix} \beta \\ \beta \\ \beta \\ 0 \\ 0 \\ 0 \end{bmatrix} \tau \tag{3.1}$$

respectively, where α is the thermal expansion coefficient, τ is the temperature increase with respect to a reference temperature T_0 for which the strain in a uniform object is taken to vanish, **p** is given in Eq. (2.2), and $\beta = dn / dT$ is the thermo-optic coefficient for a freely expanding (stress-free) object. Note that the thermo-optic contribution does not cause any birefringence, but will alter the average refractive index change.

4. Cubic layer on a large substrate

We typically are concerned about a thin layer of a cubic material like AlGaAs on a much thicker substrate. As is typically done for thermal noise calculations, we can assume that the elastic distortions of the substrate can be taken to be independent of the thin layer on its surface, and then use those distortions of the substrate as boundary conditions to compute the elastic field in the thin layer.

4.1. Layer strains in cylindrical coordinates

The in-plane displacements must be continuous at the interface of substrate and film. Assuming an axisymmetric distortion of the substrate, $u_{r,s}(r)$, then we must have in the layer $u_r(r) = u_{r,s}(r)$. If the temperature excursion in the layer is $\tau(r)$, then the displacement of the film away from its free value unconstrained by the substrate is

$$\delta u_r(r) = u_r(r) - \alpha \int_0^r \tau(r')\, dr' = u_{r,s}(r) - \alpha \int_0^r \tau(r')\, dr' \tag{4.1}$$

The strain in the film is then

$$\begin{aligned} S_{rr}(r) &= \frac{d\,\delta u_r}{dr} = S_{rr,s}(r) - \alpha\tau(r) \\ S_{\theta\theta}(r) &= \frac{\delta u_r}{r} = \frac{u_{r,s}}{r} - \alpha \frac{1}{r} \int_0^r \tau(r')\, dr' \equiv S_{\theta\theta,s}(r) - \alpha\, \Delta\tau(r) \end{aligned} \tag{4.2}$$

where the average temperature difference between the origin and a radius *r* is implicitly defined as $\Delta\tau(r)$ in the final form of Eq. (4.2). Note that for a uniform temperature field $\tau(r)=\tau_0$, the averaged temperature change takes the same value, *i.e.* $\Delta\tau(r)=\tau(r)=\tau_0$.

4.2. Layer strains in rectangular coordinates

With the transformation given in Eq. (2.19) applied to the strains given in Eqs. (4.1) and (4.2), we find for the strains in rectangular coordinates

$$\begin{aligned} S_1 &= S_{xx} = S_{xx,s} - \alpha\left[\tau\cos^2\theta + \Delta\tau\sin^2\theta\right] \\ S_2 &= S_{yy} = S_{yy,s} - \alpha\left[\tau\sin^2\theta + \Delta\tau\cos^2\theta\right] \\ S_6 &= 2S_{xy} = 2S_{xy,s} - 2\alpha(\tau-\Delta\tau)\sin\theta\cos\theta \end{aligned} \tag{4.3}$$

4.3. Thermo-optic index perturbation

For radially symmetric temperature and strain fields in a film with a free surface, the two principal refractive indexes in the layer are, with Eqs. (4.3) in Eq. (2.16)

$$\begin{aligned} n_\pm = \sqrt{\varepsilon_\pm} \approx n + \beta\tau - \frac{n^3}{2}\Bigg\{&\left[p_{11} + p_{12}\left(1 - 2\frac{c_{12}}{c_{11}}\right)\right]\left[\left(S_{1,s} + S_{2,s} - \alpha(\tau+\Delta\tau)\right)\right] \\ &\pm\sqrt{(p_{11}-p_{12})^2\left[S_{1,s} - S_{2,s} - \alpha(\tau-\Delta\tau)\cos 2\theta\right]^2 + 4p_{44}^2\left[S_{6,s} - \alpha(\tau-\Delta\tau)\sin 2\theta\right]^2}\Bigg\} \end{aligned} \tag{4.4}$$

where we have added the thermo-optic contribution to the average index change, as required by Eq. (3.1)

The birefringence is then

$$\begin{aligned} B &= -n^3\sqrt{(p_{11}-p_{12})^2\left[S_{1,s} - S_{2,s} - \alpha(\tau-\Delta\tau)\cos 2\theta\right]^2 + 4p_{44}^2\left[S_{6,s} - \alpha(\tau-\Delta\tau)\sin 2\theta\right]^2} \\ &= -n^3(p_{11}-p_{12})\sqrt{\left[S_{1,s} - S_{2,s} - \alpha(\tau-\Delta\tau)\cos 2\theta\right]^2 + A^2\left[S_{6,s} - \alpha(\tau-\Delta\tau)\sin 2\theta\right]^2} \\ &\xrightarrow[isotropic]{} -n^3(p_{11}-p_{12})\sqrt{\left[S_{1,s} - S_{2,s} - \alpha(\tau-\Delta\tau)\cos 2\theta\right]^2 + \left[S_{6,s} - \alpha(\tau-\Delta\tau)\sin 2\theta\right]^2} \end{aligned} \tag{4.5}$$

and using Eq. (2.8) a principal axis is at an angle θ_0 to **x** obeying

$$\begin{aligned} \tan 2\theta_0 &= A\frac{S_{6,s} - \alpha(\tau-\Delta\tau)\sin 2\theta}{S_{1,s} - S_{2,s} - \alpha(\tau-\Delta\tau)\cos 2\theta} \\ &\xrightarrow[isotropic]{} \frac{S_{6,s} - \alpha(\tau-\Delta\tau)\sin 2\theta}{S_{1,s} - S_{2,s} - \alpha(\tau-\Delta\tau)\cos 2\theta} \end{aligned} \tag{4.6}$$

5. Applications

5.1. Uniform temperature change

If a layer is bonded to a substrate at room temperature and then cooled to a cryogenic temperature, strains will be induced in the film if its thermal expansion coefficient α is mismatched to that of the substrate, α_s. A uniform temperature excursion the substrate, *i.e.* $\tau(r) = \tau_0 = \Delta\tau(r)$, would lead to a displacement field

$$\mathbf{u} = \alpha_s \tau_0 r \hat{\mathbf{r}} \tag{5.1}$$

neglecting a **z** displacement irrelevant here. According to Eq. (2.20) and following, the substrate strains are then $S_{1s} = S_{2s} = \alpha_s \tau_0$, $S_{6s} = 0$. According to Eq. (4.4), the index change in the film is isotropic, and given by

$$\begin{aligned} \delta n_+ = \delta n_- &= \beta\tau_0 - \frac{n^3}{2}\left[p_{11} + p_{12}\left(1 - \frac{2c_{12}}{c_{11}}\right)\right](S_{1s} + S_{2s} - 2\alpha\tau_0) \\ &= \beta\tau_0 + n^3\left[p_{11} + p_{12}\left(1 - \frac{2c_{12}}{c_{11}}\right)\right](\alpha - \alpha_s)\tau_0 \end{aligned} \tag{5.2}$$

and thus $B = 0$. This result applies equally well to cubic and isotropic layers.

5.2. Temperature rise and strain due to absorption of a Gaussian beam

For absorption of the incident optical beam by the mirror layer, there will be a radially varying temperature field in the substrate and the mirror layer, and as a result there will be a radially varying strain in the mirror layer. For beams that are large compared to the mirror layer thickness, we can estimate the strain by computing the temperature field in the substrate neglecting thermal transport in the coating, computing the resulting strain in the substrate assuming it is unaffected by the mechanical properties of the mirror layer, and then assuming the mirror layer displacements follow those of the substrate. That problem is addressed analytically for a cylindrical mirror using a Dini series solution in P. Hello and J. Y. Vinet, "Analytical models of thermal distortions in massive mirrors heated by high power laser beams," *French J. Phys.* **51**, 1267–1282 (1990). With reasonable accuracy, those results can be approximated as described in P. Lu et al, "Wavefront distortion of the reflected and diffracted beams produced by the thermoelastic deformation of a diffraction grating heated by a Gaussian laser beam," *J. Opt. Soc. Am. A* **24** pp. 659-668 (2007). When the beam is small compared to the mirror, some further simplifications are possible. When the beam is small compared to a characteristic length describing the importance of heat loss via radiation to the environment vs conduction into the substrate (discussed in following section), a simple universal form emerges for the temperature and strain fields. While detailed numerical accuracy would require FEM modeling or the use of the Hello and Vinet series results, the simple universal form here is adequate to understand the general magnitude and scaling of the problem, particularly in the central portion of the Gaussian beam.

5.2.1. Temperature and substrate displacement fields

For an incident Gaussian beam of the form $I_G(r) = I_{G0}\exp(-2r^2/w^2)$, evaluating Eq. (A8) of Lu assuming the characteristic length for surface heat loss by radiation, $l_{th} \equiv k_s/[4\varepsilon\sigma(T_0^3 - T_{ext}^3)]$, is large compared to *w*, we find for the temperature distribution at the surface of the mirror

$$\tau(r) = \tau_c\,\overline{\tau}(R) \tag{5.3}$$

where

$$\begin{aligned} \tau_c &\equiv \frac{P_{abs}}{\sqrt{2\pi}wk_s} \\ \overline{\tau}(R) &\equiv e^{-R^2}J_0(R^2) \end{aligned} \tag{5.4}$$

$R \equiv r/w$, P_{abs} is the absorbed optical power, and k_s is the thermal conductivity of the substrate, ε is the emissivity of the mirror, and σ is the Stefan-Boltzmann constant. Taking the emissivity to be 0.5, for room temperature l_{th} is 47 m for silicon, 11 m for sapphire, and 0.46 m for silica. For cryogenic temperatures, l_{th} is much larger due to the T^3 factor in the denominator, and the increase in thermal conductivity. Corrections for finite w/l_{th} are discussed in Lu.

With Eq. (B11) of Lu, we have the radial displacement in the substrate as

$$u_{r,s}(r) = u_{c,s}\,\overline{u}(R) \tag{5.5}$$

where

$$\begin{aligned} u_{c,s} &\equiv \frac{\alpha_s P_{abs}}{2\sqrt{2\pi}k_s}(1+\nu_s) \\ \overline{u}(R) &\equiv R\,e^{-R^2}\left[I_0(R^2) + I_1(R^2)\right] \end{aligned} \tag{5.6}$$

and ν_s is the substrate Poisson ratio, and I_0 and I_1 are modified Bessel functions of the first kind.

5.2.2. Substrate strain fields in cylindrical coordinates

Given the displacement field in Eq. (5.6), the strain fields in the substrate are

$$\begin{aligned} S_{rr,s} &= u_{c,s}\frac{d\overline{u}}{dr} = \frac{u_{c,s}}{w}\overline{S}_{rr}(R) \\ \overline{S}_{rr}(R) &= e^{-R^2}\left[I_0(R^2) - I_1(R^2)\right] \end{aligned} \tag{5.7}$$

and

$$\begin{aligned} S_{\theta\theta,s}(r) &= \frac{u_{r,s}}{r} = \frac{u_{c,s}}{w}\overline{S}_{\theta\theta}(R) \\ \overline{S}_{\theta\theta}(R) &\equiv e^{-R^2}\left[I_0(R^2) + I_1(R^2)\right] \end{aligned} \tag{5.8}$$

5.2.3.Substrate strain fields in rectangular coordinates

With the transformation given in Eq. (2.19) applied to the strains given in Eqs. (5.7) and (5.8), we have for the substrate strains in rectangular coordinates

$$\begin{aligned}
[S(r,\theta)] &= \frac{u_{c,s}}{w}\left[\overline{S}(R,\theta)\right] \\
\overline{S}_{1,s}(R,\theta) &= \overline{S}_{xx}(R,\theta) = e^{-R^2}\left[I_0(R^2) - I_1(R^2)\cos(2\theta)\right] \\
\overline{S}_{2,s}(R,\theta) &= \overline{S}_{yy}(R,\theta) = e^{-R^2}\left[I_0(R^2) + I_1(R^2)\cos(2\theta)\right] \\
\overline{S}_{6,s}(R,\theta) &= 2\overline{S}_{xy}(R,\theta) = -2e^{-R^2} I_1(R^2)\sin 2\theta
\end{aligned} \tag{5.9}$$

5.2.4. Photoelastic birefringence

The strains in the layer can be evaluated by substituting Eqs. (5.9) for the substrate strains and Eq. (5.4) for the temperature field into Eqs. (4.3). Those in turn lead to the layer birefringence given in Eq. (4.5) taking the form

$$\begin{aligned}
B &= -n^3\sqrt{(p_{11}-p_{12})^2\left[S_{1,s} - S_{2,s} - \alpha(\tau-\Delta\tau)\cos 2\theta\right]^2 + 4p_{44}^2\left[S_{6,s} - \alpha(\tau-\Delta\tau)\sin 2\theta\right]^2} \\
&= -2n^3\frac{u_{c,s}}{w}(p_{11}-p_{12})\left[e^{-R^2}I_1(R^2) + \frac{1}{1+\nu_s}\frac{\alpha}{\alpha_s}(\overline{\tau}-\Delta\overline{\tau})\right]\sqrt{\cos^2 2\theta + A^2\sin^2 2\theta} \\
&\xrightarrow[isotropic]{} -2n^3\frac{u_{c,s}}{w}(p_{11}-p_{12})\left[e^{-R^2}I_1(R^2) + \frac{1}{1+\nu_s}\frac{\alpha}{\alpha_s}(\overline{\tau}-\Delta\overline{\tau})\right]
\end{aligned} \tag{5.10}$$

The orientation of a principal axis is, with Eq. (4.6)

$$\theta_0 = \frac{1}{2}\tan^{-1}(A\tan 2\theta) \tag{5.11}$$

To evaluate these equations we need in addition to the temperature $\tau(r)$ the averaged temperature $\Delta\tau(r)$ defined in Eq. (4.2).

5.2.5. Application to GaAs

We can simplify Eq. (5.10) taking advantage of the large anisotropy factor in GaAs, $A^2 = 33 >> 1$ to keep only one term in the radicand. We find

$$\begin{aligned}
B &\xrightarrow[A^2\gg 1]{} -2n^3\frac{u_{c,s}}{w}(p_{11}-p_{12})A\left[e^{-R^2}I_1(R^2) + \frac{1}{1+\nu_s}\frac{\alpha}{\alpha_s}(\overline{\tau}-\Delta\overline{\tau})\right]\sin 2\theta \\
&= -\frac{1}{\sqrt{2\pi}}\frac{n^3\alpha}{k_s}\frac{P_{abs}}{w}p_{44}\left[\frac{\alpha_s}{\alpha}(1+\nu_s)e^{-R^2}I_1(R^2) + (\overline{\tau}-\Delta\overline{\tau})\right]\sin 2\theta \\
&\equiv B_0\left[\frac{\alpha_s}{\alpha}(1+\nu_s)f_s(R) + f_m(R)\right]\sin 2\theta
\end{aligned} \tag{5.12}$$

where

$$
\begin{aligned}
B_0 &\equiv -\frac{1}{\sqrt{2\pi}} \frac{n^3 p_{44} \alpha}{k_s} \frac{P_{abs}}{w} \\
f_s(R) &\equiv e^{-R^2} I_1(R^2) \\
f_m(R) &\equiv (\bar{\tau} - \Delta\bar{\tau})
\end{aligned}
\tag{5.13}
$$

The functions appearing in Eq. (5.12) are given in closed form as functions of *R*, (with $\bar{\tau} = e^{-R^2} J_0(R^2)$ from Eq. (5.4)) with the exception of $\Delta\bar{\tau}$ which is an integral given in Eq. (4.2) as

$$
\begin{aligned}
\Delta\bar{\tau}(R) &= R^{-1} \int_0^R \Delta\bar{\tau}(R')\, dR' \\
&= R^{-1} \int_0^R e^{-R'^2} J_0(R'^2)\, dR'
\end{aligned}
\tag{5.14}
$$

which must be evaluated numerically. The following is a plot of $f_m(R) = \bar{\tau}(R) - \Delta\tau(R)$ *vs R*.

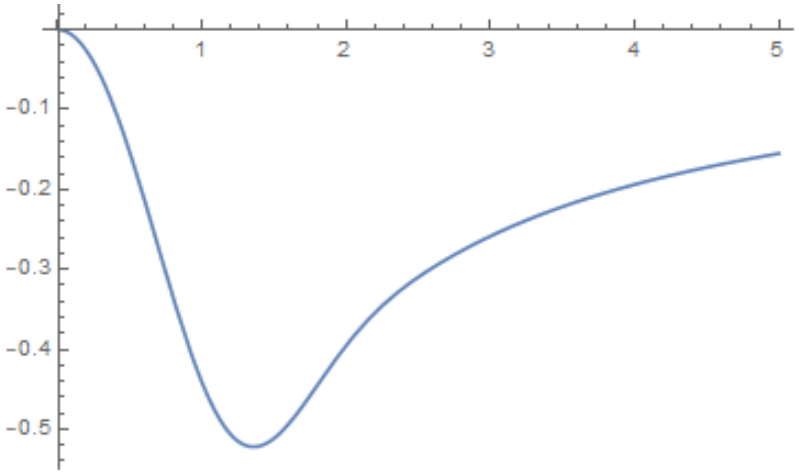

We see that $f_m(R)$ has a peak value of -0.52 at *R* = 1.38, and goes as ~0.77/*R* for $R >\sim 2$.

The other function in Eq. (5.12), $f_s(R)$, which is less important for GaAs on SiO_2 due to the latter's much smaller thermal expansion, is plotted as

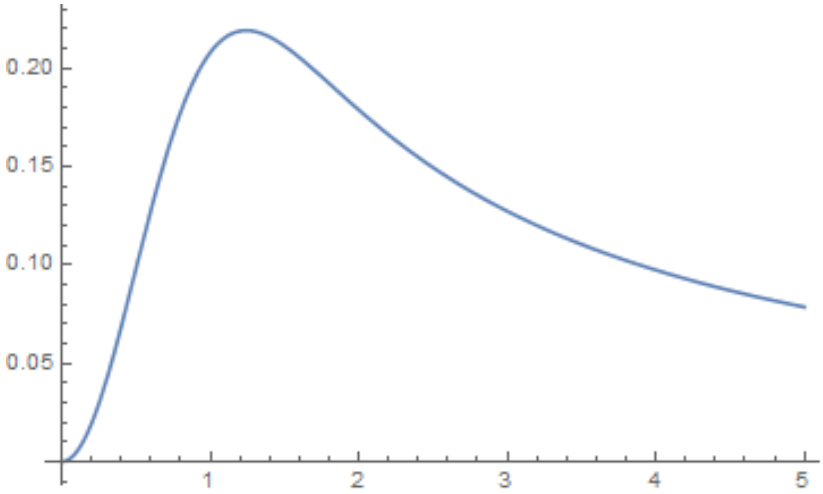

5.3. Irregular birefringence

Strains introduced during mirror growth or bonding may not be azimuthally symmetric or uniform across the face of the mirror (for example, if stick-slip motion occurs during bonding). For such cases there is no *a priori* model for the birefringence expected without knowledge of the strains. However, given a measurement of the strength and principal axes of the birefringence, one can compute the strength and principal axes of the strains that must be present to cause that birefringence, which may be of use in diagnosing and ameliorating their source. We first address the case of a single layer. The generalization to a multilayer mirror is given in section 6.4.

Assume a measurement of the birefringence B and θ_0, its principal axis orientation with respect to the crystalline **x** axis is available. We seek to compute the principal axis orientation of the strain, $\tilde{\theta}$, and the difference of the two principal strain components, $\tilde{S}_1 - \tilde{S}_2$.

We begin with Eqs. (2.9) and (2.8). Eq. (2.8) can be written as

$$A S_6 = (S_1 - S_2)\tan 2\theta_0 \tag{5.15}$$

With Eq. (5.15) in Eq. (2.9), we have for the birefringence

$$\begin{aligned} B &= -n^3(p_{11} - p_{12})(S_1 - S_2)\sqrt{1 + \tan^2 2\theta_0} \\ \Rightarrow\ S_1 - S_2 &= -\frac{B\cos 2\theta_0}{n^3(p_{11} - p_{12})} \end{aligned} \tag{5.16}$$

Eq. (5.16) in Eq. (5.15) then yields

$$S_6 = -\frac{1}{A}\frac{B\sin 2\theta_0}{n^3(p_{11} - p_{12})} = -\frac{B\sin 2\theta_0}{n^3(2p_{44})} \tag{5.17}$$

The principal axis system for the strain is the one in which the shear S_6 vanishes. Rotate the strain tensor by an angle $\tilde{\theta}$ with respect to the crystalline **x** axis. In this system, rotation of the strain tensor in the crystal axis system shows that

$$\begin{aligned} \tilde{S}_1 &= \cos^2\tilde{\theta} S_1 + \sin^2\tilde{\theta} S_2 + \cos\tilde{\theta}\sin\tilde{\theta} S_6 \\ \tilde{S}_2 &= \sin^2\tilde{\theta} S_1 + \cos^2\tilde{\theta} S_2 - \cos\tilde{\theta}\sin\tilde{\theta} S_6 \\ \tilde{S}_6 &= -2\sin\tilde{\theta}\cos\tilde{\theta} S_1 + 2\cos\tilde{\theta}\sin\tilde{\theta} S_2 + (\cos^2\tilde{\theta} - \sin^2\tilde{\theta}) S_6 \end{aligned} \tag{5.18}$$

$$\begin{aligned} \Rightarrow \tilde{S}_1 - \tilde{S}_2 &= \cos 2\tilde{\theta}(S_1 - S_2) + \sin 2\tilde{\theta} S_6 \\ \tilde{S}_6 &= -\sin 2\tilde{\theta}(S_1 - S_2) + \cos 2\tilde{\theta} S_6 \end{aligned}$$

With Eq. (5.18), we can find the principal axis orientation $\tilde{\theta}_p$ by setting $\tilde{S}_6 = 0$. We find

$$\tan 2\tilde{\theta}_p = \frac{S_6}{S_1 - S_2} = \frac{1}{A}\tan 2\theta_0 \tag{5.19}$$

where second form follows with Eq. (5.15).

To find the principal strains, begin with Eqs. (5.17) and (2.8) in Eq. (5.18):

$$\begin{aligned}\left(\tilde{S}_1 - \tilde{S}_2\right)_p &= \cos 2\tilde{\theta}_p (S_1 - S_2) + \sin 2\tilde{\theta}_p S_6 \\ &= -\frac{B\sin 2\theta_0}{n^3(2p_{44})}\sin 2\tilde{\theta}_p \left[1 + \cot 2\tilde{\theta}_p A \cot 2\theta_0\right] \\ &= -\frac{B\sin 2\theta_0}{n^3(2p_{44})}\sqrt{1 + A^2\cot^2 2\theta_0} = -\frac{B}{n^3(2p_{44})}\sqrt{\sin^2 2\theta_0 + A^2\cos^2 2\theta_0} \\ &\xrightarrow[\theta_0 \to \pi/4]{} -\frac{B}{n^3(2p_{44})}\end{aligned} \tag{5.20}$$

where second step follows from using Eq. (5.19) for $\cot 2\tilde{\theta}_p$. By similar substitutions it can be verified that $\tilde{S}_{6,p} = 0$.

Eqs. (5.19) and (5.20) are the desired relation between the measured quantities *B* and θ_0 and the principal strain magnitudes and axes. Since the birefringence is only sensitive to the difference between the principal strains, determining their absolute magnitude would require another measurement such as the phase on reflection (rather than just the difference of the phase for orthogonal polarizations) or direct strain characterization via XRD or other material characterization methods.

The case of a mirror rather than a single layer with irregular birefringence is addressed in section 6.4.

6. Multilayer mirrors

The previous analysis applies to a single uniform layer. Actual mirrors are of course comprised of a a multilayer dielectric stack. Computation of the changes in the properties of the mirror will depend on the changes in properties of each layer individually.

6.1. Refractive indexes in each layer

Tracing through the analysis for the cubic case, we see that to find the changes to the refractive index in each layer, we simply have to assign the appropriate material properties in each layer, while noting that the temperature τ, as well as the strains S_1, S_2, and S_6 are continuous through the layers, so do not require a subscript *J*. Eq. (2.15) for S_3 accounting for the free surface becomes

$$S_{3,J} - \alpha_J \tau = -\frac{c_{12,J}}{c_{11,J}}(S_1 + S_2 - 2\alpha_J \tau) \tag{6.1}$$

Eq. (2.7) for the principal refractive indexes in layer *J* becomes

$$n_{J\pm} \approx n_J - \frac{n_J^3}{2}\left\{\left[p_{11,J} + p_{12,J}\left(1 - 2\frac{c_{12,J}}{c_{11,J}}\right)\right](S_1 + S_2) \pm \sqrt{(p_{11,J} - p_{12,J})^2 (S_1 - S_2)^2 + 4p_{44,J}^2 S_6^2}\right\} \tag{6.2}$$

where the subscript *J* indicates a quantity evaluated in layer *J*.

The displacement away from its free value in each layer is modified from the form in Eq. (4.1) to

$$\delta u_{r,J}(r) = u_r(r) - \alpha_J \int_0^r \tau(r')\,dr' = u_{r,s}(r) - \alpha_J \int_0^r \tau(r')\,dr' \tag{6.3}$$

Following through to Eq. (4.4) for the principal refractive indexes in each layer

$$\begin{aligned} n_{\pm,J} \approx n_J + \beta_J \tau - \frac{n_J^3}{2}\Bigg\{&\left[p_{11,J} + p_{12,J}\left(1 - 2\frac{c_{12,J}}{c_{11,J}}\right)\right]\left[\left(S_{1,s} + S_{2,s} - \alpha_J(\tau + \Delta\tau)\right)\right] \\ &\pm\sqrt{(p_{11,J} - p_{12,J})^2\left[S_{1,s} - S_{2,s} - \alpha_J(\tau - \Delta\tau)\cos 2\theta\right]^2 + 4p_{44,J}^2\left[S_{6,s} - \alpha_J(\tau - \Delta\tau)\sin 2\theta\right]^2}\Bigg\} \end{aligned} \tag{6.4}$$

The birefringence in each layer changes from that in Eq. (4.5) to

$$\begin{aligned} B &= -n_J^3\sqrt{(p_{11,J} - p_{12,J})^2\left[S_{1,s} - S_{2,s} - \alpha_J(\tau - \Delta\tau)\cos 2\theta\right]^2 + 4p_{44,J}^2\left[S_{6,s} - \alpha_J(\tau - \Delta\tau)\sin 2\theta\right]^2} \\ &= -n_J^3(p_{11,J} - p_{12,J})\sqrt{\left[S_{1,s} - S_{2,s} - \alpha_J(\tau - \Delta\tau)\cos 2\theta\right]^2 + A_J^2\left[S_{6,s} - \alpha_J(\tau - \Delta\tau)\sin 2\theta\right]^2} \\ &\xrightarrow[isotropic]{} -n_J^3(p_{11,J} - p_{12,J})\sqrt{\left[S_{1,s} - S_{2,s} - \alpha_J(\tau - \Delta\tau)\cos 2\theta\right]^2 + \left[S_{6,s} - \alpha_J(\tau - \Delta\tau)\sin 2\theta\right]^2} \end{aligned} \tag{6.5}$$

and the orientation of the principal axis in each layer is instead of Eq. (4.6) given by

$$\begin{aligned} \tan 2\theta_{0.J} &= A_J \frac{S_{6,s} - \alpha_J(\tau - \Delta\tau)\sin 2\theta}{S_{1,s} - S_{2,s} - \alpha_J(\tau - \Delta\tau)\cos 2\theta} \\ &\xrightarrow[isotropic]{} \frac{S_{6,s} - \alpha_J(\tau - \Delta\tau)\sin 2\theta}{S_{1,s} - S_{2,s} - \alpha_J(\tau - \Delta\tau)\cos 2\theta} \end{aligned} \tag{6.6}$$

6.2. Reflection phase of the mirror stack

Changes in the reflection phase from the mirror stack due to photo-elastic effects can be calculated similarly as that from electro-optic effects. In the document "Electro-optic phase shifts in AlGaAs mirrors" it is shown that for an isotropic mirror stack, given the logarithmic derivative of the optical path length of each layer with respect to a parameter γ, *i.e.*

$$\kappa_J = \frac{1}{n_J}\frac{dn_J}{d\gamma} + \frac{dS_{3,J}}{d\gamma} \tag{6.7}$$

where S_3 is the strain in the surface normal direction, the reflectivity of a quarter-wave stack operated at the center of the reflection band is changed by

$$\left.\frac{d\phi}{d\gamma}\right|_0 \approx -\pi(n_L\kappa_H + n_H\kappa_L)\frac{n_L/n_H}{1-(n_L/n_H)^2} \tag{6.8}$$

where subscripts J = [L, H] stand for low and high index layers, respectively.

For a birefringent stack, one should in principle use, rather than the conventional 2x2 transfer matrix description, a 4x4 transfer matrix description to account for the possible polarization conversion in each layer (I believe this is given in Pochi Yeh's *Optical Waves in Layered Media* text, but I don't have it handy to check). For the present purposes, and in any case absent data for the photoelastic tensor in different AlGaAs compositions, we assume that the principal axes are aligned in each of the mirror layers, so that the conventional results for an isotropic mirror can be applied to each of the principal axes of the birefringent mirror, the important result being the difference in reflection phase for light polarized along the two principal axes.

6.3. Mirror thermoelastic birefringence.

For thermoelasticity, we take the parameter $\gamma = P_{abs}$, so that we can compute the birefringence per watt of absorbed power. With Eq. (6.8) the mirror birefringent reflection phase is then

$$\begin{aligned}
B_m &= \phi_+ - \phi_- = \left(\frac{d\phi_+}{dP_{abs}} - \frac{d\phi_-}{dP_{abs}}\right)P_{abs} \\
&= -\pi\left(\frac{n_L/n_H}{1-(n_L/n_H)^2}\right)\left[n_L(\kappa_{H+}-\kappa_{H-}) + n_H(\kappa_{L+}-\kappa_{L-})\right]P_{abs} \\
&= -\pi\left(\frac{n_L/n_H}{1-(n_L/n_H)^2}\right)\left[\frac{n_L}{n_H}\left(\frac{dn_{H+}}{dP_{abs}} - \frac{dn_{H-}}{dP_{abs}}\right) + \frac{n_H}{n_L}\left(\frac{dn_{L+}}{dP_{abs}} - \frac{dn_{L-}}{dP_{abs}}\right)\right]P_{abs} \\
&= -\pi\left(\frac{n_L/n_H}{1-(n_L/n_H)^2}\right)\left[\frac{n_L}{n_H}\frac{dB_H}{dP_{abs}} + \frac{n_H}{n_L}\frac{dB_L}{dP_{abs}}\right]P_{abs}
\end{aligned} \tag{6.9}$$

where the isotropic change in length described by S_3, drops out in the third form, and the fourth form uses the definition of the birefringence in each layer.

Eq. (6.9) can be evaluated with the expression for the birefringence from Eqs. (5.12)and (5.13). We find

$$B_m = -P_{abs}\pi\left(\frac{n_L/n_H}{1-(n_L/n_H)^2}\right)\left[\frac{n_L}{n_H}\frac{dB_{0H}}{dP_{abs}} + \frac{n_H}{n_L}\frac{dB_{0L}}{dP_{abs}}\right]\left[\frac{\alpha_s}{\alpha}(1+\nu_s)f_s(R) + f_m(R)\right]\sin 2\theta \tag{6.10}$$

The only parameters of the coating that appear in B_0 from Eq. (5.13)are α, p_{44}, and n.

6.4. Mirror with irregular birefringence

The evaluation of the principal strains and principal axes from measurements of the birefringence on reflection from a multilayer mirror can be connected to the analysis of a single layer given in section 5.3 in much the same way that the thermoelastic birefringence of a mirror was related in

section 6.3 to the single layer birefringence given in section 5.2.4. We specialize here to a quarter-wave stack, though the method is generalizable to other mirror designs.

Rewriting Eq. (6.9) for the birefringent phase in reflection for a mirror stack, in the form

$$\begin{aligned} B_m &\approx -\pi\left(\frac{n_L}{n_H}B_H + \frac{n_H}{n_L}B_L\right)\frac{n_L/n_H}{1-(n_L/n_H)^2} \\ &\approx -\pi B_H\left(1+\frac{n_L}{n_H}\right)\frac{(n_L/n_H)^2}{1-(n_L/n_H)^2} \end{aligned} \tag{6.11}$$

where the second form follows with the assumption that the photoelastic properties other than the n^3 factor are similar in the high and low index layers. With Eq. (6.11) the birefringent phase measured for the mirror stack can be related to that of the high index layer, which in turn can be related to the strain magnitude and principal axes according to Eqs.(5.19) and (5.20).

6.5. Application to AlGaAs mirrors

6.5.1. Thermoelastic birefringence

The thermal expansion coefficients of GaAs and AlGaAs appear to be similar, and I don't have data for the photoelastic coefficients of AlGaAs, so we may as well take them as the same in the two materials. In that case, Eq. (6.10) reduces to

$$B_m = B_{0m}\left[\frac{\alpha_s}{\alpha}(1+\nu_s)f_s(R) + f_m(R)\right]\sin 2\theta \tag{6.12}$$

where

$$B_{0m} \equiv -\sqrt{\frac{\pi}{2}}\frac{p_{44}\alpha}{k_s}\frac{P_{abs}}{w}\left(\frac{n_L/n_H}{1-(n_L/n_H)^2}\right)\left[n_H^2 n_L + n_L^2 n_H\right] \tag{6.13}$$

With material properties from Appendix 1, we find

$$B_m = 8.9\times10^{-3}\,\frac{P_{abs}[\mathrm{W}]}{w[\mathrm{cm}]}\left[0.11 f_s(R) + f_m(R)\right]\sin 2\theta \tag{6.14}$$

We see that for 5 W absorbed from a 5 cm radius beam, the max birefringent phase will be 4.5 mrad. Using the same scaling, if there were an absorber of 0.5 mm in size, it would create a birefringence of ~450 mrad per watt of absorbed power. Because of the weak (only $1/r$) rolloff of the birefringence away from the absorber, a larger area than that of the absorber itself would be affected.

6.5.2.Irregular birefringence

Under the same assumptions for material properties as in section 6.5.1, the relation between birefringence of reflection phase for an AlGaAs HR and the birefringence in the high index layer is

$$B_H = \frac{B_m}{18.2} \tag{6.15}$$

With Eq. (5.20) for the connection between layer birefringence and the difference between the principal strain components we have

$$\begin{aligned} \left|\tilde{S}_1 - \tilde{S}_2\right|_p &= \frac{B_H}{n_H^3 (2p_{44})} \sqrt{\sin^2 2\theta_0 + A^2 \cos^2 2\theta_0} \\ &= \frac{B_m / 18.2}{n_H^3 (2p_{44})} \sqrt{\sin^2 2\theta_0 + A^2 \cos^2 2\theta_0} \\ &= 9.3\times 10^{-6}\, B_m[\text{mrad}] \sqrt{\sin^2 2\theta_0 + A^2 \cos^2 2\theta_0} \\ &\xrightarrow[\theta_0 \to \pi/4]{} 9.3\times 10^{-6}\, B_m[\text{mrad}] \end{aligned} \tag{6.16}$$

The difference in the principal stress components corresponding to these strains will depend on the orientation of the principal axes. For the case $\theta_0 = \pi / 4$ the result is

$$\begin{aligned} \left|\tilde{T}_1 - \tilde{T}_2\right|_p &= 2c_{44} \left|\tilde{\mathrm{S}}_1 - \tilde{S}_2\right|_p \\ &\sim 1.1\text{MPa}\, B_m[\text{mrad}] \end{aligned} \tag{6.17}$$

where c_{44} = 59.4 GPa is the shear stiffness of GaAs. Note that this is the *difference* between the principal stresses – their individual magnitudes could be much larger.

7. Extensions and future work

There are several approximations involved in the results given here.

The incorporation of the stress-free surface into the strain fields of a single layer given in Eq. (2.15) was used for the individual layers of a multilayer in Eq. (6.1). Strictly speaking, this is correct only if the ratio c_{12} / c_{11} is the same in both the mirror layer materials (effectively that the Poisson ratio is the same). One could more properly evaluate the effective tetragonal-symmetry material tensors of the multilayer using the results of "Effective Thermoelastic Medium", and trace through an analysis similar to the one given here with those effective parameters, but this added complexity is perhaps worthwhile only if reliable data for the stiffness tensors and the thermal expansion coefficients vs composition of AlGaAs were available.

The thermal and strain fields for a Gaussian-distributed heat source at the surface of the mirror are simple analytical approximations, and neglect the finite diameter of the mirror compared to the beam size. The exact series results of Hello and Vinet, or FEM calculations could be used to obtain greater accuracy, but the results given here capture the scaling with absorbed power, beam size, and material parameters, and are accurate to ~20% for typical LIGO geometries, and negligibly different from more detailed calculations for beams or other heat sources small compared to the mirror diameter.

If the thermoelastic birefringence proves to be problematic for the interferometer performance, it is likely that mirror coating designs other than a simple quarter wave stack could be found to partially mitigate the problem. These however would be different from those used to eliminate thermoelastic noise, as those make use of the interplay between thermal expansion, thermo-optic and thermoelastic effects. as the former two are isotropic while the latter is birefringent, they could not fully compensate for the latter.

8. Appendix 1: Material parameters

8.1. GaAs

8.1.1. photoelastic tensor

p_{11} = -0.165, p_{22} = -0.140, p_{44} = -0.072, A = 5.76

8.1.2. thermal expansion

$\alpha = 5.73 \times 10^{-6}\ K^{-1}$

8.1.3. refractive index: $Al_xGa_{1-x}As$

$n_H(x = 0.1) = 3.45$, $n(x = 0.9) = 3.00$

8.2. Silica

$k_{th} = 1.38\ W\text{-}m^{-1}K^{-1}$

$\alpha_s = 0.55 \times 10^{-6}\ K^{-1}$

$\nu_s = 0.17$